

**MHD and Mixed convection flow near a
stagnation point over a vertical porous plate
with thermal radiation**



By
Abuzar Ghaffari

Supervised by
Dr. Tariq Javed

Department of Mathematics & Statistics
Faculty of Basic and Applied Sciences
International Islamic University, Islamabad
Pakistan, 2011

Accession No. 7H-8575

MS
SIO
ABM

1 - Mathematics

DATA ENTERED

Amz 20/06/13

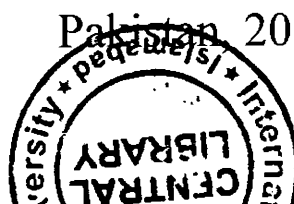
MHD and Mixed convection flow near a stagnation point over a vertical porous plate with thermal radiation



By
Abuzar Ghaffari

Department of Mathematics & Statistics
Faculty of Basic and Applied Sciences
International Islamic University, Islamabad

Pakistan 2011



MHD and Mixed convection flow near a stagnation point over a vertical porous plate with thermal radiation

By
Abuzar Ghaffari

*A Dissertation Submitted in the Partial Fulfillment of the
Requirements for the Degree of*

MASTER OF SCIENCE
In
MATHEMATICS

Supervised by
Dr. Tariq Javed

Department of Mathematics & Statistics
Faculty of Basic and Applied Sciences
International Islamic University, Islamabad
Pakistan, 2011

Dedication to my Mother

My Hero

This is a special page made especially for my Mother. She is to me my rock. She is by far the strongest woman I have ever known. She has had many trials in her life and tragedies, yet she overcomes all of them and becomes even stronger than before. I remember as I think back on hard times the strength she had. I remember always saying to her, you are so strong Ammi G , How do you do it? How do you go on? Her strength always kept her moving forward. She has been the rock for the whole family. She is there for us 100%, no questions asked.

Ammi G, words can never express the deepest gratitude I have for you. You have been there for me my whole life and I love you so much for it.

Acknowledgment

I humbly thankful to *Allah Almighty*, the Merciful and the Beneficent, who gave me health, thoughts and co-operative people to enable me, achieve this goal. I offer my humblest, sincerest and millions of Dood to the *Holy Prophet Hazrat Muhammad* (SAW), who exhorts his followers to seek for knowledge from cradle to grave.

Foremost, I would like to express my sincere gratitude to my supervisor *Dr. Tariq Javed* for the continuous support of my study and research, for his patience, motivation, enthusiasm, and immense knowledge. His guidance helped me in all the time of research and writing of this thesis. I could not have imagined having a better supervisor and mentor for my M.S (Mathematics) study.

I owe my deep gratitude and heartfelt thanks to my father *Muhammad Bashir*, who supported me throughout my career and guided me at every step in my life.

I am thankful to my fellows for the stimulating discussions for the sleepless nights we were working together before the deadline.


Last but not least, I also express thanks to my brothers, sisters, my wife little *Mahtab* and *Qasmi* for their never ending moral support and prayers which always acted as a catalyst in my academic life.

ABUZAR GHAFARI

October 20, 2011

DECLARATION

I hereby declare that this thesis, neither as a whole nor as a part thereof, has been copied out from any source. It is further declared that I have prepared this thesis entirely on the basis of my personal efforts made under the sincere guidance of my supervisor. No portion of the work, presented in this thesis, has been submitted in the support of any application for any degree or qualification of this or any other institute of learning.

Signature:  _____

Abuzar Ghaffari

MS (Mathematics)

Reg. No. 39-FBAS/MSMA/F09

Department of Mathematics and Statistics

Faculty of Basic and Applied Sciences

International Islamic university, Islamabad

Pakistan

Preface

The boundary layer from near stagnation point has several applications in engineering and technological processes and attracted many investigations during the past few decades. The pioneering work on the steady two-dimensional stagnation point flow was first initiated by Hiemenz [1], and obtained an exact similarity solution of the governing Navier-Stokes equation. Eckert [2] extended the work of [1] by considering the heat transfer analysis and presented an exact similarity solution for the thermal field. Ramachandran et al. [3] investigated the steady laminar mixed convection near a stagnation point flow around vertical plate by considering both cases of an arbitrary wall temperature and arbitrary surface heat flux variations. The problem in [1] is extended to discuss the different aspects of mixed convection flow near a stagnation point by many researchers [4-13], recently Ishak et al. [14] have studied the dual solutions in mixed convection flow near a stagnation point on a vertical porous plate. They have solved the system of nonlinear ordinary differential equation numerically using Keller-Box method [16]. Having in mind all the studies above the present dissertation is arranged as follow.

Chapter 1 includes some basic definitions and prerequisites [15] for the convenience and better understanding of the reader. The contents of the chapter 2 are based on the work of Ishak et al. [14]. All the results are reproduced with intensive care. In this chapter, Ishak et al. [14] obtained the solution of the governing nonlinear differential equation by using Keller-Box method. It is solved here in this chapter with the same method and also with shooting method [17]. It is found that shooting method also works very well for this problem too. In chapter 3, the work of Ishak et al. [14] is generalized in two different dimensions, one by introducing the Magnetohydrodynamic effects and secondly with the effects of thermal radiations. The obtained nonlinear differential equation is solved by using shooting method only. It is important to note that the dual solutions in the presence of magnetic field and thermal radiation are found. The influence of the magnetic and thermal radiation parameters are analyzed through graphs.

Contents

1 Preliminaries	4
1.1 Fluid	4
1.2 Flow	4
1.3 Fluid mechanics	4
1.4 Properties of fluid	5
1.4.1 Density	5
1.4.2 Pressure	5
1.4.3 Temperature	5
1.4.4 Viscosity	5
1.4.5 Kinematic viscosity	6
1.4.6 Specific heat	6
1.5 Classification of fluid	6
1.5.1 Ideal fluid	6
1.5.2 Real fluid	6
1.6 Types of flow	7
1.6.1 Incompressible flow	7
1.6.2 Compressible flow	8
1.6.3 Internal flow	8
1.6.4 External flow	8
1.6.5 Steady flow	8
1.6.6 Unsteady flow	8
1.6.7 Laminar flow	8

1.6.8	Turbulent flow	9
1.7	Heat transfer mechanism	9
1.7.1	Conduction	9
1.7.2	Convection	9
1.7.3	Radiation	9
1.8	Types of convection	10
1.8.1	Free or natural convection	10
1.8.2	Forced convection	10
1.8.3	Mixed convection	10
1.9	Pathlines, Streak lines, and Streamlines	10
1.9.1	Pathlines	10
1.9.2	Streak lines	10
1.9.3	Streamlines	10
1.10	Law of conservation of mass (continuity equation)	11
1.11	The momentum equation	11
1.12	Fourth-order Runge-Kutta method	12
1.13	Shooting method	13

2 Dual solutions in mixed convection flow near a stagnation point on a vertical porous plate **14**

2.1	Introduction	14
2.2	Mathematical formulation	14
2.3	Numerical solution of the boundary value problem	17
2.4	Results and discussion	19
2.4.1	Tables	19
2.4.2	Graphical representation	21
2.4.3	Discussion	22

3 MHD and Mixed convection flow near a stagnation point over a vertical porous plate with thermal radiation **24**

3.1	Introduction	24
-----	------------------------	----

3.2	Mathematical formulation	25
3.3	Results and discussion	26

Chapter 1

Preliminaries

In this chapter, some basic definitions [16] related to fluid flow, heat transfer analysis and continuity equation are introduced for the better understanding of the readers. Shooting method with Runge-Kutta 4th order integrator [17] for the general second order boundary value problem (as an example) is elaborated in detail.

1.1 Fluid

A substance sustain no fixed shape and deforms easily due to external pressure is called fluid.

1.2 Flow

A phenomenon of continuous deformation under the action of applied forces is called flow.

1.3 Fluid mechanics

A branch of engineering and physics in which we study the properties of fluid in both rest or in motion is called fluid mechanics.

1.4 Properties of fluid

1.4.1 Density

Density is mass per unit volume. In the case of fluid, we can define the density as the limit of this ratio, when a measuring volume V tends to zero. Therefore the mathematical form of density at a point is

$$\rho = \lim_{V \rightarrow 0} \left(\frac{m}{V} \right). \quad (1.1)$$

1.4.2 Pressure

Pressure p is the magnitude of the normal force F per unit area acting on a surface S . The mathematical form of pressure at a point is

$$p = \lim_{S \rightarrow 0} \left(\frac{F}{S} \right). \quad (1.2)$$

1.4.3 Temperature

Temperature is a measure of the average heat or thermal energy of the particles in a substance. Since it is an average measurement, it does not depend on the number of particles in an object. In that sense it does not depend on the size of it. *For example*, the temperature of a small cup of boiling water is the same as the temperature of a large pot of boiling water.

1.4.4 Viscosity

During the motion of the fluid, viscosity of the fluid plays an important role. Viscosity is the resistance of fluid particles against the direction of motion, it can be expressed as

$$\begin{aligned} \text{Viscosity} &= \frac{\text{Shear stress}}{\text{rate of shear strain}}, \\ \mu &= \frac{\tau_{yx}}{du/dy}. \end{aligned} \quad (1.3)$$

1.4.5 Kinematic viscosity

The Kinematic viscosity is the ratio of dynamic viscosity to density. It is denoted by ν and is defined as

$$\nu = \frac{\mu}{\rho}. \quad (1.4)$$

1.4.6 Specific heat

If the pressure is kept constant during the process, then the relation between change in temperature and heat, can be define by simple relation

$$Q = mc_p\Delta T, \quad (1.5)$$

here c_p is the specific-heat coefficient used in a constant-pressure process. If the fluid is not changing its volume during the process, then c_v is used for the specific heat in this constant-volume process

$$Q = mc_v\Delta T. \quad (1.6)$$

The ratio between these two specific-heat coefficients is denoted by

$$\gamma = \frac{c_p}{c_v}. \quad (1.7)$$

1.5 Classification of fluid

1.5.1 Ideal fluid

A fluid having zero or negligible viscosity is called ideal fluid. The occurrence of such fluid in real world is rare.

1.5.2 Real fluid

A fluid having viscosity is known as real fluid. It is denoted by μ . It is also known as viscous fluid. Real fluid is further divided into two categories.

- (i) Newtonian fluid
- (ii) Non-Newtonian fluid

Newtonian fluids

The most common fluids such as water air and gasoline are Newtonian under normal condition. The Newtonian fluids foflow the Newton Law of viscosity. If the fluid is Newtonian then

$$\tau_{yx} \propto \frac{du}{dy}. \quad (1.8)$$

The constant of proportionality in Eq. (1.8) is the absolute viscosity μ . Thus the Newton Law of viscosity is given for one dimensional flow by

$$\tau_{yx} = \mu \frac{du}{dy}. \quad (1.9)$$

Non-Newtonian fluid

The fluid in which the shear stress is not directly proportional to the deformation rate are non-Newtonian. Such fluids are further classified as having time-independent or time-dependent behavior. The non-Newtonian fluid follows the power law model. The power law model for one dimensional flow is

$$\tau_{yx} = k \left(\frac{du}{dy} \right)^n, \quad (n \neq 1) \quad (1.10)$$

where n is called the flow behavior index and the coefficient k being consistency index. It can also be written as

$$\tau_{yx} = k \left| \frac{du}{dy} \right|^{n-1} \frac{du}{dy} = \eta \frac{du}{dy}, \quad (1.11)$$

when the term $\eta = k \left| \frac{du}{dy} \right|^{n-1}$ referred to as apparent viscosity.

1.6 Types of flow

1.6.1 Incompressible flow

Flow in which variation of density is negligible is called incompressible flow. Flow of liquid is normally treated as incompressible flow.

1.6.2 Compressible flow

If the variation of density within flow is considerable then the flow is called compressible. The most common example of compressible flow is the flow of gases.

1.6.3 Internal flow

Flow completely bounded by solid surfaces, or in a pipe is called internal flow.

1.6.4 External flow

The flow of a fluid over a surface such as a plate, a wire, or a pipe is called external flow.

1.6.5 Steady flow

Fluid flow in which the properties of fluid in the domain are constant with respect to time is called steady flow. Mathematically, it can be written as

$$\frac{\partial \eta}{\partial t} = 0, \quad (1.12)$$

where η represents the fluid property that may be velocity, density, pressure etc.

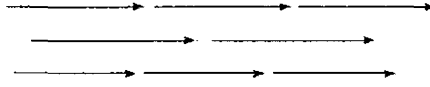
1.6.6 Unsteady flow

If the properties of the flow change with respect to time, then such a flow is called unsteady flow. Mathematically it can be represented as

$$\frac{\partial \eta}{\partial t} \neq 0. \quad (1.13)$$

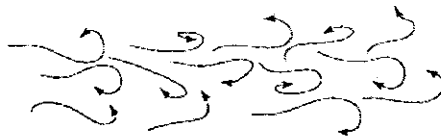
1.6.7 Laminar flow

A flow in which the fluid particles move in smooth parallel layers is called laminar flow, as shown in figure below



1.6.8 Turbulent flow

Turbulent flow is one in which the fluid particles rapidly mix with each other and not have specific path, as shown in figure below



1.7 Heat transfer mechanism

1.7.1 Conduction

The transfer of heat from one part of system to another part by inter collisions of interconnected molecules is conduction. This phenomenon occurs in solids.

1.7.2 Convection

Convection is the way in which the heat is transferred by the motion of heated molecules of the system. It usually occurs in liquids and gases.

1.7.3 Radiation

The way in which the heat is transferred by the electromagnetic waves and it does not required any medium to access the target, is known as radiation.

1.8 Types of convection

1.8.1 Free or natural convection

Natural convection is the type of heat transport in which fluid motion does not require any external agent or source to transfer its heat, it occurs only due to the difference in temperature from place to place.

1.8.2 Forced convection

If the heat transfer occurs only due to an external agent or source then this type of heat transport is called forced convection.

1.8.3 Mixed convection

If the heat transfer is due to both forced and natural convection, this phenomenon is called mixed convection.

1.9 Pathlines, Streak lines, and Streamlines

1.9.1 Pathlines

A curve describing the trajectory of a fluid element is called a pathline or a particle path.

1.9.2 Streak lines

In many cases of experimental flow visualization, particles (e.g. dye or smoke) are introduced into the flow at a fixed point in space. The line connecting all of these particles is called a streak line.

1.9.3 Streamlines

Another set of curves can be obtained (at a given time) by lines that are parallel to the local velocity vector. Mathematically describe as

$$\mathbf{V} \times d\mathbf{l} = 0, \quad (1.14)$$

\mathbf{V} is velocity vector and $d\mathbf{l}$ is streamline element.

1.10 Law of conservation of mass (continuity equation)

The rate of increase of mass in region W is equals to the rate at which mass is crossing the boundary ∂W in the inward direction, i.e.

$$\frac{d}{dt} \int_W \rho dV = - \int_{\partial W} \rho \mathbf{u} \cdot \mathbf{n} dA, \quad (1.15)$$

This is the *integral form of law of conservation of mass*. Where W be a fixed subregion of region D , ∂W denote the boundary of W , \mathbf{n} denote the unit outward normal defined at points of ∂W and let dA denote the area element on ∂W . The volume flow rate across ∂W per unit area is $\mathbf{u} \cdot \mathbf{n}$ and the mass flow rate per unit area is $\rho \mathbf{u} \cdot \mathbf{n}$. By the divergence theorem Eq. (1.15) can be written as

$$\int_W \left[\frac{\partial \rho}{\partial t} + \text{div}(\rho \mathbf{u}) \right] dV = 0, \quad (1.16)$$

and the above equation is equivalent to

$$\frac{\partial \rho}{\partial t} + \text{div}(\rho \mathbf{u}) = 0. \quad (1.17)$$

The Eq. (1.17) is the *differential form of law of conservation of mass*, also known as *continuity equation*. If ρ is constant then the continuity Eq. (1.17) reduced to

$$\nabla \cdot \mathbf{u} = 0. \quad (1.18)$$

1.11 The momentum equation

The equation of motion in vector form is

$$\rho \frac{\partial \mathbf{V}}{\partial t} = \text{div} \mathbf{T} + \rho \mathbf{b}, \quad (1.19)$$

where b is the body force per unit mass and T is the Cauchy stress tensor given by

$$\mathbf{T} = \begin{bmatrix} \tau_{xx} & \tau_{xy} & \tau_{xz} \\ \tau_{yx} & \tau_{yy} & \tau_{yz} \\ \tau_{zx} & \tau_{zy} & \tau_{zz} \end{bmatrix}, \quad (1.20)$$

where τ_{xx} , τ_{yy} and τ_{zz} are the normal stresses and τ_{xy} , τ_{xz} and τ_{zy} are the shear stresses.

1.12 Fourth-order Runge–Kutta method

Let us consider, the general equation of second order initial value problem as

$$\frac{d^2y}{dx^2} = f\left(x, y, \frac{dy}{dx}\right), \quad (1.21)$$

subject to initial conditions

$$y(x_0) = a, \quad \frac{dy}{dx}(x_0) = b. \quad (1.22)$$

In order to solve the above problem, it is required to convert the second order initial value problem to the system of two first order initial value problems by introducing new dependent variable z as

$$\left. \begin{aligned} \frac{dy}{dx} &= z = g(x, y, z), \\ \frac{dz}{dx} &= f(x, y, z), \end{aligned} \right\} \quad (1.23)$$

and the initial conditions Eq. (1.22) become

$$y(x_0) = a, \quad z(x_0) = b. \quad (1.24)$$

Now the solution of the system of two first order ordinary differential equations Eq. (1.23) subjected to initial conditions Eq. (1.24) can be computed explicitly by the formula [17]

$$y_{n+1} = y_n + \frac{1}{6}(k_1 + 2k_2 + 2k_3 + k_4), \quad (1.25)$$

$$z_{n+1} = z_n + \frac{1}{6}(l_1 + 2l_2 + 2l_3 + l_4), \quad (1.26)$$

where

$$\left. \begin{aligned}
 k_1 &= h g(x_n, y_n, z_n), \\
 l_1 &= h f(x_n, y_n, z_n), \\
 k_2 &= h g\left(x_n + \frac{h}{2}, y_n + \frac{k_1}{2}, z_n + \frac{l_1}{2}\right), \\
 l_2 &= h f\left(x_n + \frac{h}{2}, y_n + \frac{k_1}{2}, z_n + \frac{l_1}{2}\right), \\
 k_3 &= h g\left(x_n + \frac{h}{2}, y_n + \frac{k_2}{2}, z_n + \frac{l_2}{2}\right), \\
 l_3 &= h f\left(x_n + \frac{h}{2}, y_n + \frac{k_2}{2}, z_n + \frac{l_2}{2}\right), \\
 k_4 &= h g(x_n + h, y_n + k_3, z_n + l_3), \\
 l_4 &= h f(x_n + h, y_n + k_3, z_n + l_3).
 \end{aligned} \right\} \quad (1.27)$$

Where n is number of steps and h is uniform step size.

1.13 Shooting method

The simplest two-point boundary value problem is a second-order differential equation with one condition specified at $x = a$ and another one at $x = b$. Let us take in general

$$y'' = f(x, y, y'), \quad y(a) = \alpha, \quad y(b) = \beta. \quad (1.28)$$

In shooting method [17], it required to convert the given boundary value problem into the initial value problem. Boundary value problem (1.28) is reduced to an initial value problem as

$$y'' = f(x, y, y'), \quad y(a) = \alpha, \quad y'(a) = u^{(i)}. \quad (1.29)$$

Here $u^{(i)}$ is the missing initial condition needs to be determined, that could be done by assuming the value of $u^{(i)}$ as an initial guess by $u^{(0)} = s$. In this stage, our problem is to calculate the solution of initial value problem Eq. (1.29) from $x = a$ to $x = b$. The value of $y(b)$ is known at this stage, if it is to β which is our boundary condition $y(b) = \beta$, then it is ok. Otherwise we have to readjust the value of s and calculate the solution again. Mathematically instead of playing with initial guesses of $u^{(i)}$, Newton-Raphson formula is used for this purpose as follows

$$u^{(i+1)} = u^{(i)} - \frac{y(b) - \beta}{\frac{dy(b)}{dx}}.$$

Chapter 2

Dual solutions in mixed convection flow near a stagnation point on a vertical porous plate

2.1 Introduction

In this chapter, we revised the study of steady stagnation flow toward a vertical porous plate by Anuar Ishak et al. [14]. The governing system of partial differential equations is converted to system of ordinary differential equations which are then solved numerically by well-known shooting technique [17] (for two unknown initial conditions) with fourth order Runge-Kutta integration scheme and secondly by a finite-difference scheme namely the Keller-Box method [16]. The emerging features of the flow and heat transfer analysis for different ranges/values against pertinent parameters are analyzed and discussed. Both assisting and opposing flows are considered and it is similarly observed in the literature for opposing flow.

2.2 Mathematical formulation

Let us consider the flow of a viscous, incompressible fluid normal to vertical plate as a laminar two dimensional stagnation flow, as shown in Fig. 2.1. It is assumed that the vertical plate is heated with temperature $T_w(x)$, and the free stream velocity $U(x)$ and $T_w(x)$ vary linearly with

distance x with the stagnation point. Under these assumptions, the steady laminar boundary layer equations governing the flow are

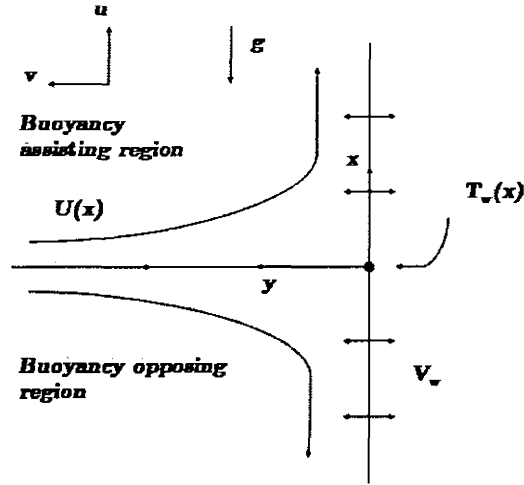


Fig. 2.1. Physical model and coordinate system

$$\frac{\partial u}{\partial x} + \frac{\partial v}{\partial y} = 0, \quad (2.1)$$

$$u \frac{\partial u}{\partial x} + v \frac{\partial u}{\partial y} = v \frac{\partial^2 u}{\partial y^2} - \frac{1}{\rho} \frac{dp}{dx} \pm g\beta(T - T_\infty), \quad (2.2)$$

$$u \frac{\partial T}{\partial x} + v \frac{\partial T}{\partial y} = \alpha \frac{\partial^2 T}{\partial y^2}, \quad (2.3)$$

subject to the boundary conditions

$$\begin{aligned} u &= 0, & v &= V_w, & T &= T_w(x) = T_\infty + bx & \text{at } y = 0, \\ u &\rightarrow U(x) = ax, & T &\rightarrow T_\infty & \text{as } y \rightarrow \infty. \end{aligned} \quad (2.4)$$

Where a and b are constants, V_w is the uniform surface mass flux, where $V_w < 0$ represents the suction and where $V_w > 0$ represents the injection, T_∞ represents ambient temperature. The last term on the right hand side of Eq. (2.2) represented with " + " and " - " signs is due to the

influence of thermal buoyancy force on the flow field pertaining to the buoyancy assisting and opposing flow regions respectively. Fig. 1 illustrates the flow field for a vertical, heated surface with the upper and lower half of the flow field being assisted and opposed by the buoyancy force respectively. By employing the Bernoulli equation in the free stream Eq. (2.2) becomes

$$U \frac{dU}{dx} = -\frac{1}{\rho} \frac{dp}{dx} \quad (2.5)$$

Eliminating dp/dx from Eq. (2.2) and Eq. (2.5) gives

$$u \frac{\partial u}{\partial x} + v \frac{\partial u}{\partial y} = \nu \frac{\partial^2 u}{\partial y^2} + U \frac{dU}{dx} \pm g\beta(T - T_\infty). \quad (2.6)$$

The introduced similarity variables are

$$\eta = \left(\frac{U}{\nu x} \right)^{\frac{1}{2}} y, \quad \psi = (U\nu x)^{\frac{1}{2}} f(\eta), \quad \theta(\eta) = (T - T_\infty)/(T_w - T_\infty), \quad (2.7)$$

where ψ is the stream function defined as $u = \partial\psi/\partial y$ and $v = -\partial\psi/\partial x$ so as to satisfy identically Eq. (2.1). After using Eq. (2.7), we get the following ordinary differential equations:

$$f''' + ff'' + 1 - f'^2 + \lambda\theta = 0, \quad (2.8)$$

$$\frac{1}{Pr}\theta'' + f\theta' - f'\theta = 0, \quad (2.9)$$

where prime denotes the derivative with respect to η , $Pr = \frac{\nu}{\alpha}$ is the Prandtl number and $\lambda = \pm Gr_x/Re_x^2$ is the mixed convection parameter where \pm sign has the same meanings as in Eq. (2.2). Where in the above expression $Gr_x = g\beta(T_w - T_\infty)x^3/\nu^2$ and $Re_x = Ux/\nu$ are local Grashof and local Reynolds number respectively. $\lambda > 0$ corresponds to the assisting flow and if $\lambda < 0$ corresponds to opposing flow when $\lambda = 0$, the flow is lacking in buoyancy force, it is for pure forced convection flow. The boundary conditions from Eq. (2.4) now become

$$\begin{aligned} f(0) &= f_0, \quad f'(0) = 0, \quad \theta(0) = 1, \\ f'(\infty) &\rightarrow 1, \quad \theta(\infty) \rightarrow 0. \end{aligned} \quad (2.10)$$

Where $f_0 = f(0) = -\frac{V_w}{(\nu a)^{1/2}}$ is a constant with $f_0 > 0$ is for mass suction and $f_0 < 0$ is for mass injection, while $f_0 = 0$ means impermeable plate. It is worth mentioning that when $f_0 = 0$, Eqs. (2.8 – 2.10) reduce to those formed by Ramachandran et al. [3], for the case of an arbitrary surface temperature with $n = 1$ in their paper. The physical quantities of interest are skin friction coefficient C_f and the local nusselt number Nu_x , which are defined as

$$C_f = \frac{\tau_w}{\frac{1}{2}\rho u_\infty^2}, \quad (2.11)$$

$$Nu_x = \frac{xq_w}{k(T_w - T_\infty)}. \quad (2.12)$$

Where the skin friction τ_w and heat transfer from the plate q_w are given by

$$\tau_w = \mu \left(\frac{\partial u}{\partial y} \right)_{y=0} \quad \text{and} \quad q_w = -k \left(\frac{\partial T}{\partial y} \right)_{y=0}, \quad (2.13)$$

with μ and k being the dynamic viscosity and thermal conductivity respectively. After using the similarity variables Eq. (2.7), we get

$$\frac{1}{2}C_f Re_x^{1/2} = f''(0), \quad Nu_x / Re_x^{1/2} = -\theta'(0). \quad (2.14)$$

2.3 Numerical solution of the boundary value problem

Since the boundary value problem Eqs. (2.8 – 2.10) is non-linear, so it is impossible to find its analytical exact solution. Now we use Numerical scheme shooting method with Runge-Kutta fourth order integrator and implicit finite difference scheme (Keller-Box) to construct its solution. For both used scheme we need to convert modeled system of boundary value problem

to the first order initial value system as follows

$$\left. \begin{aligned}
 f &= y_1, \\
 f' &= y_2, \\
 f'' &= y_3, \\
 y_3' &= -y_1 y_3 - 1 + (y_2)^2 - \lambda y_4, \\
 \theta &= y_4, \\
 \theta' &= y_5, \\
 \text{and } y_5' &= (y_2 y_4 - y_1 y_5) Pr,
 \end{aligned} \right\} \quad (2.15)$$

with initial conditions

$$\begin{aligned}
 y_1(0) &= f_0, \quad y_2(0) = 0, \quad y_3(0) = u_1, \\
 y_4(0) &= 1, \quad y_5(0) = u_2.
 \end{aligned} \quad (2.16)$$

Where u_1 and u_2 are two unknown missing conditions. The missing conditions can be found in such a way that solution satisfy the boundary conditions (2.10). We construct the solution both with the help of implicit finite difference scheme [16] and shooting method [17] up to the accuracy of 10^{-6} . It is observed that, since Eq. (2.8) and (2.9) carry coupled nonlinear ordinary differential equations, missing initial conditions and the value of infinity are highly dependent on the physical parameters λ , Pr and f_0 . It is assured that the solution obtained by both scheme are highly accurate with each other and the value of missing initial conditions are calculated with great care.

2.4 Results and discussion

2.4.1 Tables

Table 1: Values of $f''(0)$ for different values of Pr when $\lambda = 1$ and $f_0 = 0$.

Pr	Ramachandran et al. [3]	Hassanien et al. [12]	Lok et al. [13]	Result by [14]	
				Upper branch	Lower branch
0.7	1.7063	1.70632	1.7064	1.7063	1.2387
1	–	–	–	1.6754	1.1332
7	1.5179	–	1.5180	1.5179	0.5824
10	–	1.49284	–	1.4928	0.4928
20	1.4485	–	1.4486	1.4485	0.3436
40	1.4101	–	1.4102	1.4101	0.2111
50	–	1.40686	–	1.3989	0.1720
60	1.3903	–	1.3903	1.3903	0.1413
80	1.3774	–	1.3773	1.3774	0.0947
100	1.3680	1.38471	1.3677	1.3680	0.0601

Table 2: Values of $-\theta'(0)$ for different values of Pr when $\lambda = 1$ and $f_0 = 0$.

Pr	Ramachandran et al. [3]	Hassanien et al. [12]	Lok et al. [13]	Result by [14]	
				Upper branch	Lower branch
0.7	0.7641	0.76406	0.7641	0.7641	1.0226
1	—	—	—	0.8708	1.1691
7	1.7224	—	1.7226	1.7224	2.2192
10	—	1.94461	—	1.9446	2.4940
20	2.4576	—	2.4577	2.4576	3.1646
40	3.1011	—	3.1023	3.1011	3.1080
50	—	3.34882	—	3.3415	4.4976
60	3.5514	—	3.5560	3.5514	4.8572
80	3.9095	—	3.9195	3.9095	5.5166
100	4.2116	4.23372	4.2289	4.2116	6.1230

Table 3: The coordinates of the bifurcation points $(\lambda_c, f''(0))$ and $(\lambda_c, -\theta'(0))$ as shown in Figs. 2.2–2.5.

Pr	f_0	$(\lambda_c, f''(0))$	$(\lambda_c, -\theta'(0))$
1	-0.5	(-1.6049, -0.1681)	(-1.6049, 0.1935)
	0	(-2.3618, -0.4036)	(-2.3618, 0.4092)
	0.5	(-3.6629, -0.8251)	(-3.6629, 0.6935)
10	0	(-4.0363, -0.4186)	(-4.0363, 0.9457)

2.4.2 Graphical representation

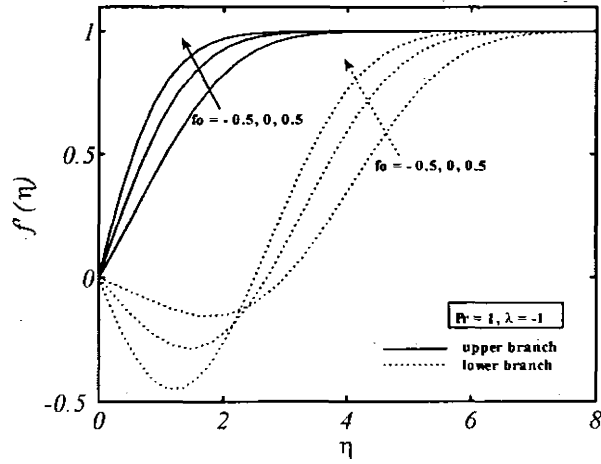


Fig. 2.2: Effects on velocity profiles for different values of f_0 when $Pr = 1$ and $\lambda = -1$ (opposing flow).

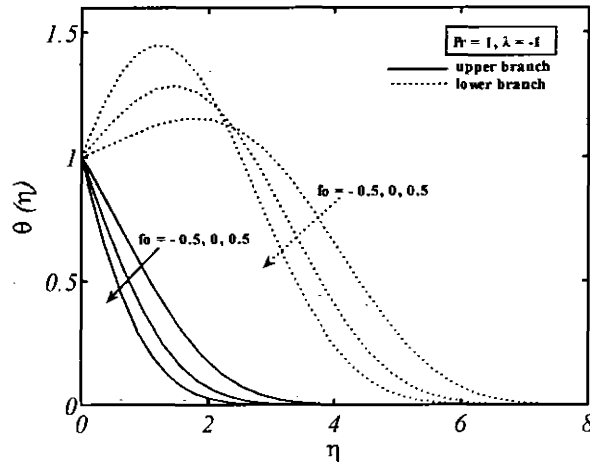


Fig. 2.3: Effects on temperature profiles for different values of f_0 when $Pr = 1$ and $\lambda = -1$ (opposing flow).

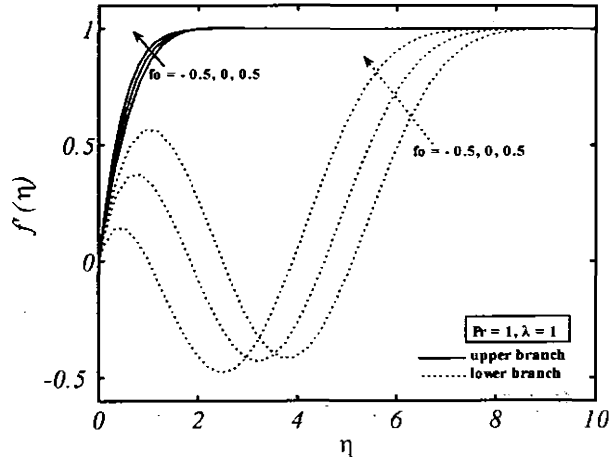


Fig. 2.4: Effects on velocity profiles for different values of f_0 when $Pr = 1$ and $\lambda = 1$ (assisting flow).

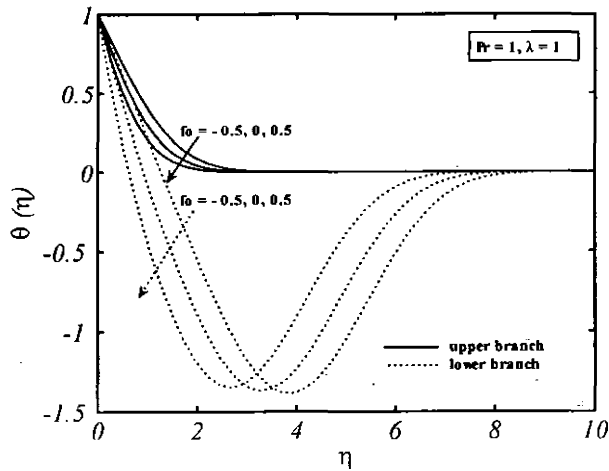


Fig. 2.5: Effects on temperature profiles for different values of f_0 when $Pr = 1$ and $\lambda = 1$ (assisting flow).

2.4.3 Discussion

The coupled ordinary differential equations Eq. (2.8) and (2.9) subject to the boundary conditions Eq. (2.10) are solved numerically using the shooting scheme with fourth order Runge-Kutta method as an integrator to solve the initial value problem and secondly by using an

implicit finite difference scheme known as Keller-Box method as described in the book of Cebeci and Bradshaw [16]. In order to validate the results, Tables 1–3 of [14] are reproduced exactly. Tables 1 and 2 are constructed to compare the values of skin friction coefficient $f''(0)$ and local nusselt number $-\theta'(0)$ with the results available in the paper of Ramachandran et al. [3], Hassanien and Gorla [12], Devi et al. [6] and Lok et al. [8, 13]. It is seen that the results reproduced are in good agreement. It is observed through Figs. 2.2–2.5 (dotted line) that the dual solutions exist for both the opposing and assisting flows. The coordinates of bifurcation points, where the lower branch solution and upper branch solution coincide with each other are shown in Table 3. It is observed that for $\lambda > \lambda_c$, there is no solution. It is required to find the solution for this range, complete Navier-Stokes equations needs to be solved. Figs. 2.2 and 2.3 illustrate the effects of velocity and temperature profiles when $\lambda = -1$ (for the opposing flow) and Figures 2.4 and 2.5 are for $\lambda = 1$ (for the assisting flow). In all of the figures, the solid and dashed lines are for the upper branch and lower branch solutions respectively. For $\lambda = -1$ (see Fig. 2.2). The velocity profiles for the upper branch solution increases especially near the wall, while they are decreasing for the lower branch solution for all values of f_0 considered for figure. It is to be remembered that $f_0 > 0$ represent suction and $f_0 < 0$ represent injection. However, for the assisting flow when $\lambda > 0$, the velocity increases near the wall for both upper branch and lower solution as shown in Fig. 2.4. It is interesting to note that reversed flow occurs as $f''(0) < 0$ for $\lambda = 1$ and $\lambda = -1$ for the lower branch solutions. Fig. 2.3 shows the effects of different value of f_0 on temperature profile. It is seen that the temperature decreases near the wall when f_0 take its values from negative to positive. It is interesting that temperature profile remain positive for both upper and lower branch solution as compared to Fig. 2.5 where, for lower branch solution, the temperature profile become negative which has no physical meaning at all.

Chapter 3

MHD and Mixed convection flow near a stagnation point over a vertical porous plate with thermal radiation

3.1 Introduction

In this chapter we study the effect of magnetohydrodynamics (MHD) and thermal radiation effect on a mixed convection flow near a stagnation point on a vertical porous plate. We introduce MHD and thermal radiation in the problem which have been studied in last chapter. The governing partial differential equations are converted to ordinary differential equation with the same similarity variables introduced in chapter 2 given by [14], which are then solved by well-known shooting technique (for two unknown initial conditions) with fourth order Runge-Kutta integration scheme. The solution is obtained for different values of pertinent parameters involved in the problem. It is observed the dual solution exist even in the presence of MHD and thermal radiation effects. Ranges of the parameters, for which the dual solution exist are calculated and drawn very carefully.

3.2 Mathematical formulation

We consider steady two dimensional and incompressible electrically conducting fluid past over a porous vertical plate. A constant magnetic field of strength B_0 is applied perpendicular to the plate. The induced magnetic field is neglected due to the assumption of small magnetic Reynold number. Under these assumptions, the continuity equation, law of conservation of momentum and energy equation are given as

$$\frac{\partial u}{\partial x} + \frac{\partial v}{\partial y} = 0, \quad (3.1)$$

$$u \frac{\partial u}{\partial x} + v \frac{\partial u}{\partial y} = \nu \frac{\partial^2 u}{\partial y^2} + U \frac{dU}{dx} \pm g\beta(T - T_\infty) - \frac{\sigma B_0^2 u}{\rho}, \quad (3.2)$$

$$u \frac{\partial T}{\partial x} + v \frac{\partial T}{\partial y} = \frac{k}{\rho c_p} \frac{\partial^2 T}{\partial y^2} - \frac{1}{\rho c_p} \frac{\partial q_r}{\partial y}, \quad (3.3)$$

subject to the same boundary conditions as define in previous chapter Eq. (2.4). Here σ is the electrical conductivity of the fluid and q_r is the radiative heat flux. The radiative heat flux q_r is defined as

$$q_r = -\frac{4\sigma^* \partial \bar{T}^4}{3k^* \partial y}, \quad (3.4)$$

where σ^* and k^* are the Stefan-Boltzmann constant and the Rosseland mean absorption coefficient respectively. We assume that the temperature differences within flow is such that the term T^4 may be expressed as a linear function of temperature. Hence, expanding T^4 by Taylor series about T_∞ (the fluid temperature in the free stream) and neglecting higher-order terms, we get

$$T^4 \cong 4T_\infty^3 T - 3T_\infty^4. \quad (3.5)$$

In view of Eq. (3.4) and (3.5), the Eq. (3.3) reduces to

$$u \frac{\partial T}{\partial x} + v \frac{\partial T}{\partial y} = \left(\alpha + \frac{16\sigma^* T^3}{3\rho c_p k^*} \right) \frac{\partial^2 T}{\partial y^2}. \quad (3.6)$$

Where $\alpha = k/\rho c_p$ is the thermal diffusivity. From the above equation, it is seen that the effect of radiation is to enhance the thermal diffusivity. If we take $N_r = \frac{kk^*}{4\sigma^* T_\infty^3}$ as the radiation

parameter, Eq. (3.6) becomes

$$u \frac{\partial T}{\partial x} + v \frac{\partial T}{\partial y} = \frac{\alpha}{k_0} \frac{\partial^2 T}{\partial y^2}, \quad (3.7)$$

where $k_0 = \frac{3N_r}{3N_r+4}$. After introducing the same similarity variables Eq. (2.7) define in chapter 2, Eqs. (3.2) and (3.7) reduced to the form

$$f''' + f f'' - f'^2 - M^2 f' + 1 + \lambda \theta = 0, \quad (3.8)$$

$$\frac{1}{k_0 Pr} \theta'' + f \theta' - f' \theta = 0, \quad (3.9)$$

where k_0 , the thermal radiation and M , the magnetic field. It is important to mention here that for $k_0 = 1$, thermal radiation effects are not considered. Where $\lambda = \pm Gr_x / Re_x^2$ is the mixed convection parameter and $Gr_x = g\beta(T_w - T_\infty)x^3/v^2$ and $Re_x = Ux/v$ are Grashof and Reynolds numbers respectively. The solution of the above coupled equations Eqs. (3.8) and (3.9) are highly dependent on λ , due to its property that it is responsible for the coupling of these two nonlinear differential equations. In this chapter too, $\lambda > 0$ and $\lambda < 0$ correspond to the assisting and opposing flows respectively and $\lambda = 0$ means no convection. The boundary conditions for Eqs. (3.8) and (3.9) remain same as given in Eq. (2.10). In this chapter, the solution of the boundary value problem Eqs. (3.8) and (3.9) subject to the boundary conditions (2.10) has only been carried out by using shooting method.

3.3 Results and discussion

The variation in skin-friction coefficient $f''(0)$ and the local Nusselt number $-\theta'(0)$ against λ , for different values of f_0 ($f_0 = 0$, $f_0 = 0.5$ and $f_0 = -0.5$) and for Prandtl number $Pr = 1$, magnetic field $M = 0.5$ and radiation parameter $N_r = 0.7$ are presented in Figs. 3.1 and 3.2. While the comparison of results between $Pr = 1$ and $Pr = 10$ for $f_0 = 0$ (impermeable wall) and for magnetic field $M = 0.5$ and radiation parameter $N_r = 0.7$ are presented in Figs. 3.3 and 3.4.

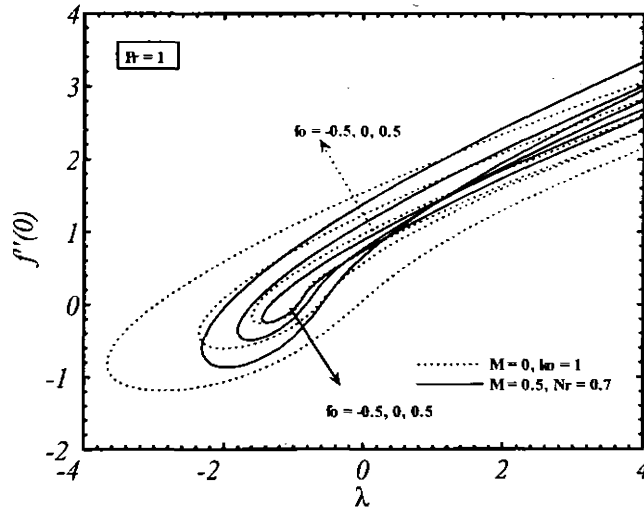


Fig. 3.1: Effects of skin friction coefficient $f''(0)$ as a function of λ for the different values of f_0 when $Pr = 1$, $M = 0.5$ and $N_r = 0.7$

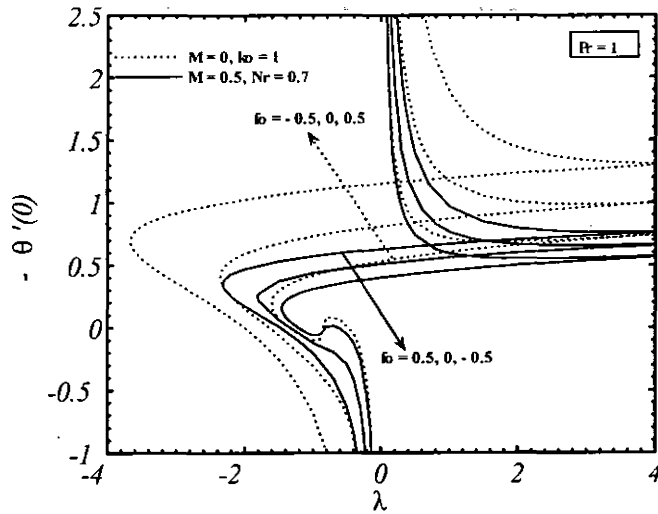


Fig. 3.2 Effects of local nusselt number $-\theta'(0)$ as a function of λ for the different values of f_0 when $Pr = 1$, $M = 0.5$ and $N_r = 0.7$.

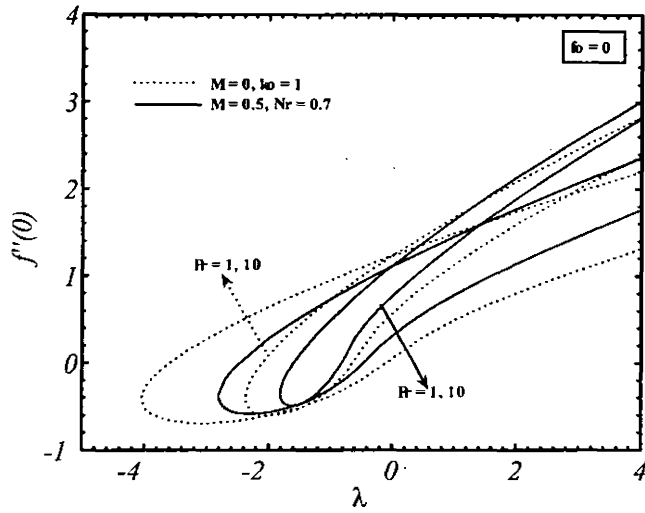


Fig. 3.3: Effects of skin friction coefficient $f''(0)$ as a function of λ for $Pr = 1$ and $Pr = 10$ when $f_0 = 0$, $M = 0.5$ and $N_r = 0.7$.

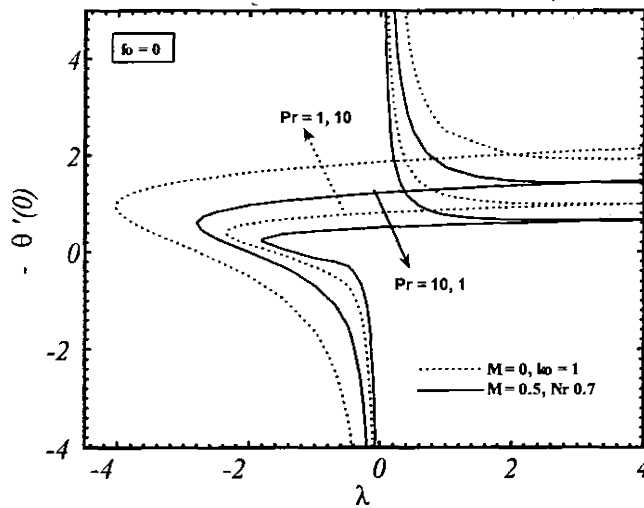


Fig. 3.4: Effects of local nusselt number $-\theta'(0)$ as a function of λ for $Pr = 1$ and $Pr = 10$ when $f_0 = 0$, $M = 0.5$ and $N_r = 0.7$.

Figs. 3.5 and 3.6 show the velocity and temperature profile for $\lambda = 1$, while for $\lambda = -1$, velocity and temperature profiles are shown in Figs. 3.7 and 3.8 for Prandtl number, $Pr = 1$

magnetic field, $M = 0.1$ and radiation parameter, $N_r = 0.7$.

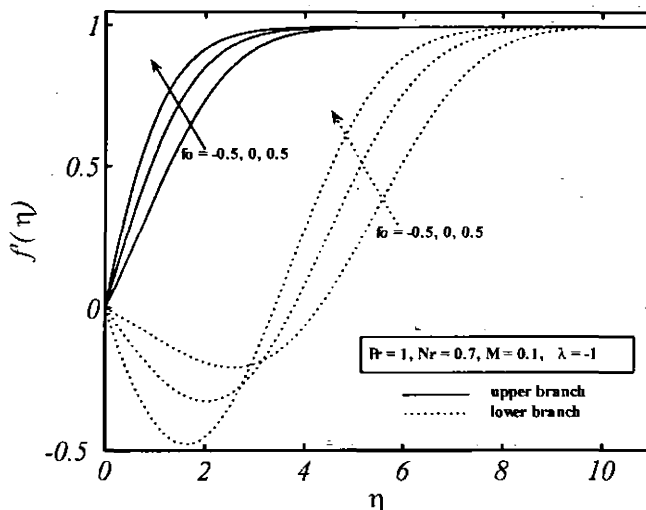


Fig. 3.5: Effects on velocity profiles for different value of f_0 when $Pr = 1$ and $\lambda = -1$ (opposing flow), $Nr = 0.7$ and $M = 0.1$ with $f_0 > 0$ for suction and $f_0 < 0$ for injection.

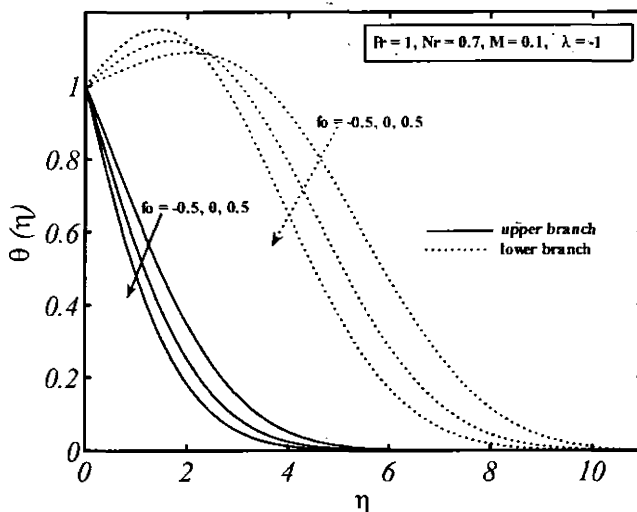


Fig. 3.6: Effects on temperature profiles for different values of f_0 when $Pr = 1$ and $\lambda = -1$ (opposing flow), $Nr = 0.7$ and $M = 0.1$ with $f_0 > 0$ for suction and $f_0 < 0$ for injection.

74-8575

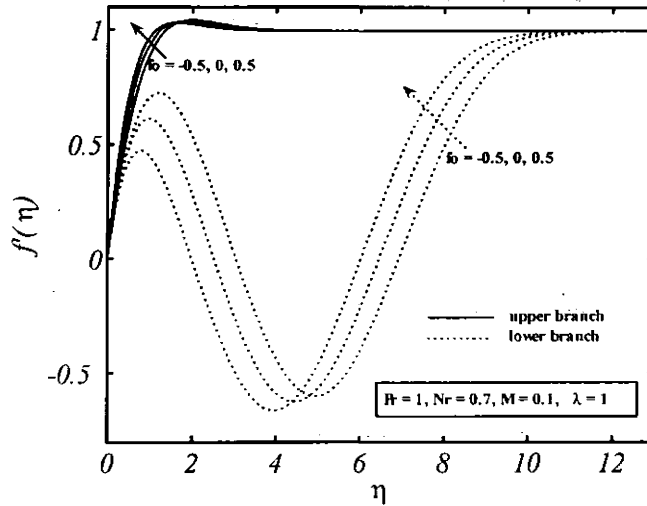


Fig. 3.7: Effects on velocity profiles for different values of f_0 when $Pr = 1$ and $\lambda = 1$ (assisting flow), $Nr = 0.7$ and $M = 0.1$ with $f_0 > 0$ for suction and $f_0 < 0$ for injection.

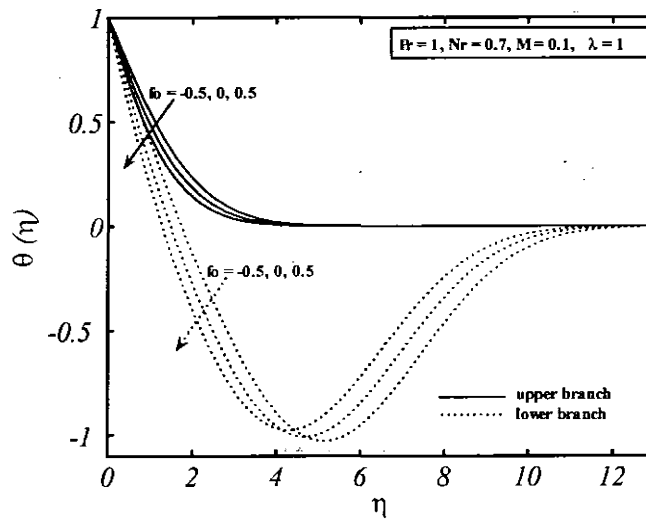


Fig. 3.8: Effects on temperature profiles for different values of f_0 when $Pr = 1$ and $\lambda = -1$ (assisting flow), $Nr = 0.7$ and $M = 0.1$ with $f_0 > 0$ for suction and $f_0 < 0$ for injection.

The effects of the buoyancy parameter λ for $f_0 = -0.5$ (injection), $f_0 = 0$ (impermeable wall) and $f_0 = 0.5$ (suction) on the skin friction coefficient $f''(0)$ and the local nusselt number

$-\theta'(0)$ are shown in Figures 3.1 and 3.2 respectively, Figures 3.3 and 3.4 show the effects of the comparison of the results between $Pr = 1$, and $Pr = 10$ on the skin friction coefficient $f''(0)$ and the local nusselt number $-\theta'(0)$ respectively. It is important to note that dashed lines represent results when the magnetic parameter (M) and the radiation parameter (Nr) are kept absent and solid lines represent the data, when $M = 0.5$ and $Nr = 0.7$. These figures infer the existence of the dual solution for the assisting flow ($\lambda > 0$) and opposing flow ($\lambda < 0$) that have already been represented by Ramachandran et al. [3], Devi et al. [6] and Lok et al. [8, 13]. It is worth mentioning here that, in the presence of magnetic field and radiation effects, there exist dual solution too. For $\lambda > 0$, there is a favorable pressure gradient due to the buoyancy forces, where the results in flow being accelerated for this range of the parameters and consequently there is a large skin friction coefficient than in the non-buoyant case ($\lambda = 0$). For $\lambda < 0$, there is a critical value of λ_c . There exist dual solution when $\lambda > \lambda_c$ and a saddle-node bifurcation when $\lambda = \lambda_c$, and no solution when $\lambda < \lambda_c$. For $\lambda = \lambda_c$, the boundary layer separate from the surface. Therefore, it is not possible to get the solution for $\lambda < \lambda_c$ by the using the boundary layer approximation. To obtain the solution for $\lambda < \lambda_c$, the complete Navier-Stokes equations has to be solved. It can easily be observed from Fig. 3.1 that the range of parameter λ for which the dual solution exist become reduced with the presence the magnetic field M . As the value of λ_c is almost near to -3.6 when $M = 0$, and now it reduces to near -2.2 for $f_0 = 0.5$ when $M = 0.5$, similarly for $f_0 = 0$, for impermeable case, λ_c reduces from near -2.3 to -1.8 and for $f_0 = -0.5$, λ_c reduces from -1.6 to -1.5 . Similarly observation is made from Fig. 3.2. It is observed from Figs. 3.1 and 3.3 that the lower branch solution has a lower value of $f''(0)$ for a given λ than the upper branch solution, even when the magnetic field is present. It is noticed that the boundary layer thickness reduces, when the magnetic field is applied, and is valid for all values of f_0 and Pr . These figures also show that the magnitude of the critical value $|\lambda_c|$ increases as the injection or suction parameter f_0 as well as prandtl number Pr is increased in the presence of magnetic field and radiation effects too. Figs. 3.2 and 3.4 are drawn to show the effects of local nusselt number $-\theta'(0)$ due to λ for different values of f_0 and Pr . For $M = 0$, $k_0 = \frac{3Nr}{3Nr+4} = 1$ and $M \neq 0$, $k_0 = \frac{3Nr}{3Nr+4} \neq 1$, represents dashed lines and solid lines respectively. These figures suggest that as soon $\lambda \rightarrow 0^-$ or $\lambda \rightarrow 0^+$, the value of $-\theta'(0)$ for lower branch solution becomes unbounded. It is also observed that the value of $|\theta'(0)|$, local

nusselt number minimizes when the magnetic field and the radiation effects are applied. Figs. 3.5 to 3.8 are drawn to show the influences of these pertinent parameters f_0 , λ , M and k_0 in the velocity and temperature profiles. All these figures support the existence of dual solution as shown in Figs. 3.1 to 3.4.

Bibliography

- [1] K. Hiemenz, Die Grenzschicht an einem in den gleichförmigen Flüssigkeitsstrom eingetauchten geraden Kreiszyylinder, *Dingl. Polytech. J.* 32 (1911) 321–410.
- [2] E. R. G. Eckert, Die Berechnung des Wärmeübergangs in der laminaren Grenzschicht umstromter Körper, *VDI Forschungsheft* 416 (1942) 1–23.
- [3] N. Ramachandran, T. S. Chen, B. F. Armaly, Mixed convection in stagnation flows adjacent to a vertical surfaces, *ASME J. Heat Transfer*, 110 (1988) 373–377.
- [4] F. R. de Hoog, B. Laminger and R. Weiss, A numerical study of similarity solutions for combined forced and free convection, *Acta Mech.* 51 (1984) 139–149.
- [5] N. Afzal and T. Hussain, Mixed convection over a horizontal plate, *ASME J. Heat Transfer*, 106 (1984) 240–241.
- [6] C. D. S. Devi, H. S. Takhar and G. Nath, Unsteady mixed convection flow in stagnation region adjacent to a vertical surface, *Heat Mass Transfer*, 26 (1991) 71–79.
- [7] A. Ridha, Aiding flows non-unique similarity solutions of mixed-convection boundary-layer equations, *J. Appl. Math. Phys. (ZAMP)*, 47 (1996) 341–352.
- [8] Y. Y. Lok, N. Amin, D. Campean and I. Pop, Steady mixed convection flow of a micropolar fluid near the stagnation point on a vertical surface, *Int. J. Numerical Methods Heat Fluid Flow*, 15 (2005) 654–670.
- [9] A. Ishak, R. Nazar, N. Bachok, and I. Pop, MHD mixed convection flow near the stagnation-point on a vertical permeable surface, *Physica A: Statistical Mechanics and its Applications*, 389 (2010) 40–46.

- [10] A. Ishak, R. Nazar, and I. Pop, Dual solutions in mixed convection flow near a stagnation-point on a vertical surface in a porous medium, *Int. J. Heat and Mass Transfer*, 51 (2008) 1150-1155.
- [11] R. Nazar, N. Amin, I. Pop, Unsteady mixed convection boundary layer flow near the stagnation point on a vertical surface in a porous medium, *Int. J. Heat Mass Transfer*, 47 (2004) 2681-2688.
- [12] I. A. Hassanien, R. S. R. Gorla, Combined forced and free convection in stagnation flow of micropolar fluid over vertical non-isothermal surface, *Int. J. Engng. Sci.* 28 (1990) 783-792.
- [13] Y. Y. Lok, N. Amin, and I. Pop, Unsteady mixed convection flow of a micropolar fluid near the stagnation point on a vertical surface, *Int. J. Thermal Sci.* 45 (2006) 1149-1157.
- [14] A. Ishak, R. Nazar, N. M. Arfin and I. Pop, Dual solutions in mixed convection flow near a stagnation-point on a vertical porous plate, *Int. J. Thermal Science*, 47 (2008) 417-422.
- [15] H. Schlichting, K. Gersten, *Boundary layer theory*, 8th Edition, Springer.
- [16] T. Cebeci, P. Bradshaw, *Physical and Computational Aspects of Convective Heat Transfer*, New York, 1988, Springer-Verlag.
- [17] T. Y. Na, *Computational methods in Engineering boundary value problems*, 1979, Academic Press.